MALAYSIAN JOURNAL OF ANALYTICAL SCIENCES

Journal homepage: https://mjas.analis.com.my/

Research Article

Synthesis, biological evaluation and molecular docking analysis of *p*-tolyldiazenyl azo derivatives

Kai Wei Yeo[1], Ainaa Nadiah Abd Halim[1*], Nor Hisam Zamakshshari[1], Surisa Phornvillay[1], Zainab Ngaini[1], Davlye Noissy Diosing[1], Akshatha Handattu Shankaranarayana[2], and B. R. Prashantha Kumar[2]

[1]Faculty of Resource Science and Technology, Universiti Malaysia Sarawak, 94300 Kota Samarahan, Sarawak, Malaysia
[2]Department of Pharmaceutical Chemistry, JSS College of Pharmacy, Sri Shivarathreeshwara Nagar, Mysuru-570015, India

[*]Corresponding author: ahanadiah@unimas.my

Received: 29 August 2024; Revised: 19 November 2024; Accepted: 3 December 2024; Published: 27 June 2025

Abstract
Impacts of multiresistant bacteria such as *Staphylococcus aureus* and *Escherichia coli* have initiated active research of new effective drugs. Herein, new *p*-tolyldiazenyl azo derivatives **1-13** were successfully synthesized through a well-established diazo coupling reaction of *p*-toluidine with substituted phenol at *ortho*, *meta* and *para* positions. The series was obtained in a moderate yield of 58% – 79% and structural elucidation was done using FTIR and NMR spectroscopies. The antioxidant ability of the compounds **1-13** evaluated by 2,2'-diphenyl-1-picrylhydrazyl (DPPH) and ferric reducing antioxidant power (FRAP) assay outlined a potential activity with IC_{50} of 26 – 188 ppm and 12.29 – 182.73 mg/mL Trolox equivalent, respectively. Moreover, the antibacterial activity of the compounds assessed *via* the Kirby-Bauer disc diffusion method against *S.aureus* and *E.coli* show moderate to good inhibition zone of 7.04±0.50 mm to 17.46±0.50 mm as compared to standard ampicillin (19.29±0.33 mm). Determination of minimum inhibitory concentration (MIC) through a turbidimetric method towards similar bacteria strains, gave a MIC values of 84 – 178 ppm (*S.aureus*) and 112 – 194 ppm (*E.coli*) with compound **3** (*m*-F) (84.37 ppm) and **9** (*m*-Br) (112.40 ppm) are better than ampicillin which the MIC were 97.70 ppm and 112.92 ppm for *S.aureus* and *E.coli* respectively. The molecular docking analysis towards MurE and DHFR enzymes reveals that the hydrogen bonding, hydrophobic and electrostatic interactions with amino acid in the vicinity are the major contributions to the activities. This study is important in discovering a potentially new candidate for combating emerging infections.

Keywords: diazotisation, C-coupling, antioxidant, antibacterial, MIC

Introduction

Antibiotics were considered as most astonishing medical discovery in the 20th century [1]. However, the abuse and imprudent of antibiotics usage in various sectors have contributed to the natural evolution of gene mutation that facilitates antimicrobial resistance [2,3]. The rapid emergence of multidrug-resistant bacteria has been a serious life-threatening issue for global public health due to the misuse of antibiotics [4,5] with a projection of 10 million deaths per year by 2050 [6]. Other than the adverse effect on the healthcare sector, acid-producing bacteria such as *S. aureus* and *E. coli* play their parts in initiating 20% of corrosion globally, which mostly influences the oil and gas industry, water pipelines and clinical settings [7]. It was estimated to be approximately an annual loss of USD 2.5 trillion to the world economy due to the microbially influenced corrosion sparked by organic acid secreted from microbes' metabolism process [8,9].

Due to that, the investment and research and development of new synthetic drugs against antimicrobial resistance have been intensified whereby a nitrogen-containing molecule specifically azo moiety is being seen as a potential scaffold by the researcher [10]. This is owing to its cost-effectiveness [11], simplicity [12] and reproducibility of the synthetic procedure [13] in addition to well-established pharmaceutical applications [14]. The incorporation of azo moiety as the nitrogen-containing group into a new compound acts as a bridge linkage and enhances the synergic effect

[15,16]. Its unique properties such as flexibility [17], easy uptake by substrate [18], push-pull characteristic [19] and thermal stability [20] have given the moiety major attention. Azo compounds are traditionally used as dyes in textile industries [21], biomedical [22] and food industries [14]. Balsalazide, sulfasalazine, and olsalazine are examples of established drugs for colorectal diseases such as inflammatory bowel diseases [23,24] and colon cancer [25] treatments. These azo-bonded drugs' ability to act as a hypoxia-responsive linker was resulting from their proficiency in reducing and cleaving the reductive species such as azoreductase [26] that would be able to deliver the drug to the targeted organ at the lower gastrointestinal tract [27]. Hence, azo as part of hypoxia-responsive agent and glutathione (GSH-responsive agent) often used in hypoxia imaging and tumor targeting treatment [28].

Azo moieties can be synthesized from the diazotization of the amine group and coupled with phenol making the *p*-toluidine a suitable precursor for the development of new azo compounds. Over the years, *p*-toluidine has been used in the manufacturing of various pharmaceutical drug synthesis, pesticides and dyes such as *p*-toluidine-*m*-sulfonic acid and *m*-nitro-*p*-toluidine [29]. A recent study by Obasuyi and Iyekowa (2019) also utilized *p*-toluidine in a synthesis of a Schiff base compound with antibacterial activity. Despite that, the studies on the *p*-toluidine azophenol derivatives for biological properties specifically for both antibacterial and antioxidant activities are still limited and seldomly reported. In this context, the azo moiety is expected to contribute to antibacterial properties as it can be protonated under acidic conditions to interact with the phosphate group of the bacterial cell wall leading to an interruption of cell membrane formation [31]. Whereas, the presence of a hydroxyl group able to donate the hydrogen atom and form a chemical bonding [32,33] apart from extended π electron conjugation and tautomeric form of azo-hydrazo structure [34] is potentially attributed to antioxidant activity. The synergistic approach by combining different functional groups in a single structure is envisaged to enhance the biological potential *via* the ability to target multiple active sites and different mechanisms of pathogens [35].

Herein, this study aims to incorporate azo moieties from the diazo coupling reaction of *p*-toluidine with phenol derivatives as a promising alternative for multidrug-resistant bacteria and antioxidant properties due to their synergistic effect [15,16]. The antioxidant capacity of compounds **1-13** was screened through DPPH and FRAP assay while the antibacterial activities were evaluated using Kirby Bauer disc diffusion and turbidimetric kinetic methods. Furthermore, *in silico* molecular docking analysis towards dihydrofolate reductase (DHFR) and UDP-N-acetylmuramyl-tripeptide synthetase (MurE) enzymes defined the interactions occurring attributed to the eminent antibacterial activities of synthesized compounds.

Materials and Methods

Measurement and reagents

The solvents and reagents used were obtained from Merck and employed without further purification. The melting point of the compounds was determined using an open tube capillary (Stuart SMP3). The Thermo Scientific^{TM} FLASH 2000 analyzers are used for the CHN analysis. The presence of functional groups was identified *via* an FTIR spectra analyzer (Perkin Elmer Thermoscientific Smart Omni Transmission Nicolet 1605 Spectrophotometer). An NMR spectrometer (JOEL ECA 500) was used to record ^{1}H (500 MHz) and ^{13}C (125 MHz) NMR spectra in DMSO- d_6 and chemical shifts were reported in δ ppm. A UV-visible spectrophotometer (Shimadzu UV-1900i) was used to perform optical measurements.

Synthesis of *p*-tolyldiazenyl azo derivatives (1-13)

The *p*-toluidine (2 mmol) was dissolved in the mixture of water (10 mL) and HCl (6 mL, 3M) before being cooled to a low temperature (0-5 ˚C) under ice bath conditions. Dissolved sodium nitrite (10 mL) was added to the mixture to form diazonium salt which was closely monitored by potassium iodide paper for 10-15 minutes until the KI paper turned blue. Phenol derivative (2 mmol) was subsequently added to the diazonium salt under alkaline conditions. The pH of the solution was adjusted to pH 8-9 to form a stable product. The reaction was under continuous stirring for the following 15 minutes and closely monitored by thin-layer chromatography (TLC) [36]. A few drops of 50% HCl were added to induce the precipitation of the product. Filtration was then performed to obtain a crude solid compound with further purification *via* recrystallisation using methanol: water (ratio 1:15).

Antioxidant evaluation

DPPH free radical scavenging assay

Freshly prepared 2,2-diphenyl-2-pycrylhydrazine (DPPH) (0.00394g) was dissolved in methanol (100 mL) prior to being added into synthesized compounds at various concentrations (200 ppm, 100 ppm, 50 ppm, 25 ppm, 12.5 ppm and 6.25 ppm). The solution mixture was incubated in the

dark for 0.5 hour before taking the absorbance reading using the UV-VIS spectrophotometer at 517 nm. Ascorbic acid was employed as standard drug while methanol was used as negative control. The scavenging activity (%) of the compounds was calculated using the following formula:

$$\text{Scavenging activity } \% = \frac{(A_C - A_t)}{A_t} \text{ x } 100\%$$

Where,
A_C = Absorbance reading of negative control after 30 minutes
A_t = Absorbance reading of tested compound after 30 minutes

A graph with scavenging activity (%) versus concentration (ppm) was plotted to determine the scavenging activity value (IC_{50}) of the synthesized compounds.

Ferric reducing antioxidant power (FRAP) assay

A fresh FRAP reagent comprising of 0.1M of acetate buffer at pH 3.6, 10 mM of 2,4,6-tripyridylstriazine (TPTZ) in 40 mM of HCl and 20 mM of iron (III) chloride ($FeCl_3$) with a ratio of 10:1:1 was prepared. The FRAP reagent (1.9 mL) was added to 100 µL of sample at 2 ppm in a vial. Ascorbic acid was employed as standard while methanol was used as a negative control. The aqueous mixture was incubated in the dark before the absorbance being measured using a UV-VIS spectrophotometer at 593 nm. The calibration curve of Trolox was used as a standard [37]. The reducing power of the compounds was derived from the standard graph and expressed as the equivalent amount of milligram of Trolox equivalents milligram per milliliter.

Antibacterial activity

Kirby-Bauer disc diffusion method

The antibacterial activity of the compounds was screened with the Kirby-Bauer disc diffusion method [38]. Mueller-Hinton broth was used to grow Gram-positive bacteria (*Staphylococcus Aureus*, ATCC 25923) and Gram-negative bacteria (*Escherichia coli*, ATCC 25922) for 18 hours at 37°C and 120 rpm. McFarland turbidity ($1x10^8$ CFU/mL) of inoculum was measured as standard before being spread on agar [39]. A sterile cotton bud was used to spread the inoculum containing bacteria (100 µL) and later were left to dry. Each disk comprising the impregnated compound at a concentration of 100 ppm (10 µL) was pressed softly to ensure full contact with the agar surface. The bacterial plates were then incubated for 24 hours. The zone of inhibition was measured, and the mean value and standard deviation were calculated. The procedure was done in triplicates to improve the accuracy and reliability of the result. The result was compared to ampicillin as positive control in this experiment while DMSO was employed as a negative control.

Minimum inhibitory concentration (MIC)

The bacteriostatic potential of the compounds was tested *via* the turbidimetric kinetic method by employing gram-positive bacteria (*Staphylococcus Aureus*, ATCC 25923) and gram-negative bacteria (*Escherichia coli*, ATCC 25922) [36]. The bacteria were cultured in Luria-Bertani broth for 24 hours under optimum conditions at 120 rpm. The Luria-Bertani broth (10 mL) was added with different concentrations of compounds (50 ppm, 80 ppm and 100 ppm) and 0.2 mL of inoculums. The mixture was shaken for 6 hours by using an incubator. Then, 1 mL of aliquots of each concentration was pipetted out into a cuvette at every interval of 1 hour to monitor the transmittance value (T). The transmittance reading was taken using a UV-visible spectrophotometer Shimadzu (UV-1900i) at a wavelength of 560 nm. The values obtained were substituted into the Equation 1 and 2 according to the bacteria strain to the determination of In N_t which indicates the number of colonies forming unit (CFU) mL^{-1} against time.

$$\textit{S. aureus} : \text{In } N_t = 27.4 - 10.3T \quad \text{(Eq. 1)}$$
$$\textit{E. coli} : \text{In } N_t = 27.1 - 8.56T \quad \text{(Eq. 2)}$$

Next, the values obtained were subjected to Equation 3 to obtain a specific growth rate of bacteria when µ=0. The graph on specific growth rate versus concentration was plotted and extrapolated to identify the minimum inhibitory concentration (MIC).

$$\mu = (\text{In } N_t - \text{In } N_0)/(t - t_0) \quad \text{(Eq. 3)}$$

Molecular docking

The crystal structure of UDP-N-acetylmuramyl-tripeptide synthetase (MurE) from *E.coli* crystalized with co-crystal ligand N-[2-(2,5-dioxopyrrolidin-1-yl)ethyl]-3-methylbenzamide (PDB ID: 7B6M, Ligand ID: SZN) and Exogenous Dihydrofolate Reductase (DHFR) from *S. aureus* complexed with Trimethoprim (PDB ID: 2W9S, Ligand ID: TOP) were downloaded from the Protein Data Bank (RCSB-PDB website). Maestro 2023-3 (version: 13.7.125) interface of Schrodinger was used for all the steps involved in Molecular Docking studies. The proteins were prepared following

Maestro's Protein Preparation module [40] by removing the EDO ligand and chain A away in 7B6M. Whereas, in 2W9S, ligands NDP and GOL, chains B, C, D and E were removed. In addition, the water molecules in both proteins that are not critical and out of the binding site were also removed to ensure binding scores accuracy [41,42]. While generating a receptor grid, the SZN and TOP ligands were picked as the binding sites for the respective protein with the cubic grid box size of 24 Å and receptor grid centers (*x*, *y*, *z*) set at [6.619, –0.014, 40.248] and [–37.031, 5.202, 0.727], respectively, as determined using the Receptor Grid Generation module. The active site key residues involved in grid generation included VAL184, SER202, LEU189, THR115, PHE204, LEU207, VAL245, TRP249, HOH779, HIS232, and CYS234 for the SZN-binding protein and ASN18, SER49, THR46, VAL6, ILE5, ALA7, ASP27, LEU20, PHE92, TYR98, and ILE31 for the TOP-binding protein. The synthesized compounds (ligand) were prepared using the LigPrep module of Schrodinger with default settings. The Glide module of the Schrodinger suit was then used to dock the prepared ligands to the binding sites with default settings of Standard Precision (SP) mode [43]. The docking scores obtained for the ligands were compared with the docking scores of the cocrystal and ampicillin (standard reference). The 2D interaction diagrams of docked complexes were visualized using the Discovery Studio 2024 Visualizer.

In silico ADMET pharmacokinetic prediction

An online tool, pkCSM, was employed to increase the accuracy and efficiency of identifying new drugs. The analysis involves a SMILES string of the compound structure to predict the absorption (A), distribution (D), metabolism (M), excretion (E) and toxicity (T) of the compounds. The deep comprehension of the compound through the pkCSM is able to reduce the deviations between clinical and laboratory tests and less adverse effects through the employment of computational technology during the drug development test [44].

Results and Discussion

Chemistry

The *p*-toluidine as starting material was dissolved in hydrochloric acid and distilled water to react with sodium nitrite to obtain a series of *p*-tolyldiazenyl azo derivatives **1-13** under ice bath condition (0–5 ºC) for 15 minutes to form diazonium benzene chloride salt. The formation was confirmed by using potassium iodide paper which turned purple [45]. The synthesis was done under low temperatures due to the highly reactive and unstable condition of the diazonium salt which can easily decompose [46–48]. The *p*-toluidine was used as the starting material due to the presence of methyl group at the *para*-position that acts as an electron donating group and would be able to increase the basicity of nitrogen atoms that expedite the protonation forming interaction with bacteria [49,50]. The phenol derivatives as coupling reagents in sodium hydroxide were added to the priorly prepared arenediazonium salt intermediate. The reaction progress was constantly checked through TLC before being acidified with a few drops of concentrated hydrochloric acid to obtain a moderate yield of 52% –78% of targeted compounds **1**–**13** after recrystallisation. The synthesis route is illustrated as shown in **Scheme 1.1**

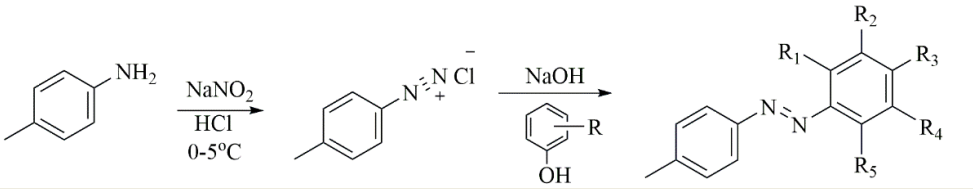

Compound	R_1	R_2	R_3	R_4	R_5	Compound	R_1	R_2	R_3	R_4	R_5
1	H	H	OH	H	H	**8**	H	Br	OH	H	H
2	H	F	OH	H	H	**9**	Br	H	OH	H	H
3	F	H	OH	H	H	**10**	H	Br	H	H	OH
4	H	F	H	H	OH	**11**	H	OCH_3	OH	H	H
5	H	Cl	OH	H	H	**12**	OCH_3	H	OH	H	H
6	Cl	H	OH	H	H	**13**	H	OCH_3	H	H	OH
7	H	Cl	H	H	OH						

Scheme 1.1 Synthesis route of *p*-tolyldiazenyl azo derivatives **1-13**

The structural elucidation of the synthesized compounds was done by using FTIR and NMR spectroscopic analyses. In the FTIR spectra, strong absorption bands were observed at 1474-1502 cm^{-1} indicating the presence of the N=N bond [51] which confirmed the azo formation. The presence of a peak at frequencies 3021 – 3261 cm^{-1} was attributed to the ν_{OH}, while the C=C skeleton of aromatic rings corresponded to the absorption band at 1520–1605 cm^{-1} [52,53]. In the ^{1}H NMR, one singlet peak was observed at most downfield of 10.25 – 11.07 ppm corresponding to the O-H, while another one singlet peak was observed at the most upfield attributed to the methyl (-CH_3) peak. The presence of hydroxyl proton was assigned to the most downfield peak due to the formation of hydrogen bonds between the OH group with electron-rich acceptors that deplete the electron density and result in highly deshielding nuclei [54]. The deshielding phenomenon was created by the external magnetic field that flows along with the direction of the induced magnetic field during the π-electrons rotation in a clockwise direction leading to an increase in the effective magnetic field experienced by the nuclei [55]. Despite that, the hydroxyl group on compound **8** (*o*-Br) was not detected due to the labile proton property resulting from the rapid exchange of respective protons [56]. Meanwhile, the multiple peaks detected from the range of 6.45 ppm to 7.92 ppm were assigned to protons from the aromatic ring. On the other hand, the ^{13}C NMR analysis showed the presence of a C-O peak at most downfield regions of 150.25 – 162.34 ppm except for compounds **2**, **3** and **4** with fluoro-substituted compounds had a C-F peak at the most downfield instead. This finding is due to the more electronegativity of fluorine atoms as compared to oxygen, resulting in a highly deshielding effect [57,58]. The peaks at 99.83 – 141.45 ppm were attributed to carbon in the aromatic ring while the peak observed at the most upfield region corresponded to the methyl group.

Antioxidant evaluation

Given the structural composition of compounds **1-13**, the presence of the phenolic group is highly associated with antioxidant activity due to its ability to donate a hydrogen atom to reduce the free radical species [59].

DPPH free radical scavenging assay

DPPH is a colorimetric method [60] whereby the antioxidant ability of the compound is indicated by the decolorization of the purple color of the DPPH solution. The decolorization to pale yellow occurred due to the cability of the compound to transfer hydrogen atoms to form hydrazine derivatives [61] *via* hydrogen atom transfer (HAT) and single atom transfer (SET) mechanisms [62]. In this study, the compounds were dissolved and prepared at different concentrations (6.25 ppm, 12.50 ppm, 25 ppm, 50 ppm, 100 ppm and 200 ppm) before being added to the DPPH solution. The absorbance reading of the mixture was measured at 517 nm wavelength after 30 minutes of incubation in the dark. Ascorbic acid was used as a standard for result comparison while methanol was employed as negative control. The half-maximal inhibitory concentration (IC_{50}) effectively reduced by the synthesized compounds is tabulated in **Table 1**. The IC_{50} can be interpreted as an effective concentration of the compound to reduce the initial concentration of DPPH by 50% [63].

Based on the analysis, compounds **1-13** showed a wide range of antioxidant properties with IC_{50} of 25.5 ppm to 187.8 ppm, which mainly contributed by the presence of a phenolic functional group and extended π-electron conjugated species from the compound structure [64,65]. Comparatively, *ortho*-substituted compounds have shown higher antioxidant activity across the series. The result is aligned with a previous study which reported that *ortho*-substituted compounds have higher antioxidant ability than *para*- and *meta*-substituted compounds [54]. Significantly, compound **11** (*o*-OCH_3) showed the highest antioxidant potential with IC_{50} of 25.5 ppm. This result is possibly due to the presence of the methoxy group at the *ortho* position, which lowers the ionization potential, resulting in an easier dissociation of hydrogen atoms from the OH group [66]. Ascorbic acid showed higher antioxidant activity than all the compounds tested, as the structure of the compound has more than one hydroxyl group [67].

Ferric reducing antioxidant power (FRAP) assay

Other than the DPPH assay, the colorimetric FRAP assay was also conducted by monitoring the color change of the solution from pale yellow (ferri-tripyridyl-triazine [Fe(III)TPTZ] complex) to blue (ferro-tripyridyl-triazine [Fe(II)TPTZ]) measure at 593 nm [68–70]. This method relies on the ability of the antioxidant to reduce the Fe(III) complex to the Fe(II) complex *via* a single electron transfer (SET) mechanism in an acidic medium to maintain the solubility of the complex [71]. The results obtained were tabulated as shown in **Table 2**.

Table 1. Effective inhibition concentration IC_{50} of compound **1-13**

Compound	Value IC_{50} (ppm)	Compound	Value IC_{50} (ppm)
1 (H)	44.5	**8** (*o*-Br)	74.5
2 (*o*-F)	39.0	**9** (*m*-Br)	>200
3 (*m*-F)	42.2	**10** (*p*-Br)	>200
4 (*p*-F)	187.8	**11** (*o*-OCH_3)	25.5
5 (*o*-Cl)	29.1	**12** (*m*-OCH_3)	>200
6 (*m*-Cl)	31.2	**13** (*p*-OCH_3)	>200
7 (*p*-Cl)	35.6	**Ascorbic Acid**	17.8

The results from FRAP analysis showed that compounds **1** (H), **2** (*o*-F), **8** (*o*-Br), **11** (*o*-OCH_3), **12** (*m*-OCH_3) and **13** (*p*-OCH_3) have outperformed the antioxidant activity of the standard ascorbic acid. In general, compounds with *ortho*- or *para*- of methoxy compound showed excellent activity due to their resonance and inductive effects [72]. The exceptional antioxidant activity of the methoxy series could be due to the ability of the methoxy group to reduce the O-H bond dissociation enthalpy which consequently reduces the stability of phenoxy radicals of the compound [73]. Other than that, the electron-donating behavior of the methoxy increased the electronic effect [74], electron cloud density [54] and HOMO energy that contributed to higher antioxidant activity [75,76]. On the other hand, the lower antioxidant properties of the halogenated compound might be due to the higher electron transfer enthalpy value and proton affinity [77].

Antibacterial activity

Kirby-Bauer disk diffusion method

Kirby-Bauer disk diffusion was carried out to screen the antibacterial property of the compound by employing the McFarland turbidity standard to standardize the number of bacteria in the broth suspension before it (100 µL) was spread evenly on the Mueller-Hinton agar plates [78,79]. Compounds were tested against Gram-positive bacteria (*Staphylococcus aureus*) and Gram-negative bacteria (*Escherichia coli*) with ampicillin chosen as positive control while DMSO alternately was employed as the negative control. The zone of inhibition was measured after 24 hours of incubation and the results obtained were tabulated as in **Table 3**.

Generally, all compounds tested against *S. aureus* exhibited satisfying antibacterial activity except for compound **11** (*o*-OCH_3). The inactivity of **11** (*o*-OCH_3) might be due to steric hindrance caused by the presence of the hydroxyl group next to the methoxy [100,101]. Whereas, the potential showed by the most halogenated substituted compounds owing to improved lipophilicity given by the ability of the compound to withdraw electron density away from the conjugated system [82], which consequently enhance binding ability towards the targeted molecular binding site hence increasing the antibacterial activity [83]. The overall results were also found to be more susceptible to *S. aureus* compared to *E. coli* which was believed to be due to the difference in the cell wall composition of the two strains. In gram-negative bacteria, the presence of lipopolysaccharides in the cell membrane protects the membrane from chemical attacks [84]. The complex outer membrane of *E. coli* consists of oligosaccharides, proteins and lipids that are capable of repelling both hydrophobic and hydrophilic molecules which improves the resistance of gram-negative bacteria [85]. On the other hand, *S. aureus*, a gram-positive bacteria composed of a simpler cell wall structure with a lack of outer cell membranes comprised of just cytoplasmic lipid membrane and layers of cross-linked peptidoglycan [86,87] is more fragile to penetration. The excellent antibacterial activity is owing to the existence of a hydroxyl group that effectively formed hydrogen bonding with the lipid bilayers, causing the rupture of bacteria cell walls leading to disruption of the arrangement and permeability mechanism of microsomes, lysosomes, and bacterial walls [88,89].

Minimum inhibitory concentration (MIC)

The bacteriostatic potential of compounds **1-13** was further examined with a turbidimetric kinetic method to determine the minimum inhibitory concentration (MIC). MIC is denoted as the lowest concentration of a compound that is capable of suppressing the growth of bacteria tested under controlled conditions [90]. In this study, the bacteriostatic potential of the compounds was evaluated at 50 ppm, 80 ppm and 100 ppm against the same bacteria strains of *S. aureus* and *E. coli*, whereby the growth of

bacterial rate was monitored through UV-VIS spectrophotometer for every interval hour. The transmittance values obtained were then calculated for the number of colonies forming (CFU/mL) and the specific growth rate of bacteria was tabulated as in the supplementary material file. Thereafter, MIC values were determined by extrapolating the graph of specific growth rate versus concentration as in shown **S76-77** with all the values summarized in **Table 4**.

Table 2. Trolox equivalent of compound **1-13**

Compound	FRAP (mg Trolox Eq mg/ml)	Compound	FRAP (mg Trolox Eq mg/ml)
1 (H)	71.66	**8** (*o*-Br)	77.86
2 (*o*-F)	76.52	**9** (*m*-Br)	14.11
3 (*m*-F)	15.69	**10** (*p*-Br)	65.57
4 (*p*-F)	12.29	**11** (*o*-OCH_3)	106.32
5 (*o*-Cl)	57.42	**12** (*m*-OCH_3)	87.66
6 (*m*-Cl)	41.85	**13** (*p*-OCH_3)	182.73
7 (*p*-Cl)	27.49	**Ascorbic Acid**	70.43

Table 3. Zone of inhibition of compound **1-13**

Compound	Diameter of Inhibition Zone (mm)		Compound	Diameter of Inhibition Zone (mm)	
	E. coli	***S. aureus***		***E. coli***	***S. aureus***
1 (H)	6.21±0.26	15.25±0.34	**9** (*m*-Br)	7.04±0.50	18.75±0.34
2 (*o*-F)	6.79±0.26	14.92±0.67	**10** (*p*-Br)	6.50±0.00	6.60±0.33
3 (*m*-F)	6.63±0.22	17.46±0.50	**11** (*o*-OCH_3)	6.17±0.24	-
4 (*p*-F)	6.46±0.54	6.33±0.25	**12** (*m*-OCH_3)	6.25±0.34	10.83±0.75
5 (*o*-Cl)	6.29±0.26	16.71±0.26	**13** (*p*-OCH_3)	6.33±0.25	6.21±0.26
6 (*m*-Cl)	6.50±0.00	15.96±0.14	**Ampicillin**	18.21±0.40	19.29±0.33
7 (*p*-Cl)	6.50±0.00	15.79±0.26	**DMSO**	-	-
8 (*o*-Br)	6.25±0.26	6.67±0.44			

Note: (-) = no activity; *o* = ortho, *m* = meta, *p* = para

Table 4. Minimum inhibitory concentration of **1-13**

Compound	Concentration (ppm)		Compound	Concentration (ppm)	
	E. coli	***S. aureus***		***E. coli***	***S. aureus***
1 (H)	>200.00	143.99	**9** (*m*-Br)	112.40	103.95
2 (*o*-F)	193.68	158.84	**10** (*p*-Br)	>200.00	>200.00
3 (*m*-F)	171.19	84.37	**11** (*o*-OCH_3)	>200.00	>200.00
4 (*p*-F)	191.55	>200.00	**12** (*m*-OCH_3)	>200.00	169.45
5 (*o*-Cl)	>200.00	110.36	**13** (*p*-OCH_3)	>200.00	>200.00
6 (*m*-Cl)	182.79	104.55	**Ampicillin**	112.92	95.70
7 (*p*-Cl)	>200.00	162.95	**DMSO**	-	-
8 (*o*-Br)	>200.00	178.20			

Note: (-) = no activity; *o* = ortho, *m* = meta, *p* = para

The result tabulated showed a similar trend as in Kirby-Bauer screening with halogen-bearing compounds **2–10** having better inhibitory action than methoxylated compounds **11–13** remarkably the *meta*-substituted toward *S. aureus*. This result has suggested that the *meta*-substituted electron withdrawing group improve the binding affinity of compounds towards the bacteria [91], resulting from the electron deficiency and higher hydrophobicity of compounds [74] that enhance the bacteriostatic potential. In addition, the halogen atom elevates the binding linearity of the compound *via* non-covalent halogen bond interactions providing better membrane permeabilization activity and catabolic stability [92–94]. However, it is worth noting that the presence of different halogenated substituents on the compounds plays an important role in determining the conformations of molecules binding to the active site of bacteria in correspondence to steric, lipophilic, binding ability and cell membrane solubilities [95]. Notably, compound **3** (*m*-F) showed the lowest MIC (84.37 ppm) indicating the highest antibacterial potential against gram-positive bacteria instead of compound **9** (*m*-Br) despite having the largest inhibition zone of 18.75±0.34 mm in the disc diffusion screening earlier. The contradicting result could be due to the smaller fluoro atom granting a bigger inductive effect led to a larger dipole moment and strengthening of scavenging activity [96,97]. The larger the dipole moment, the stronger the antibacterial potential [98]. Nevertheless, compound **9** (*m*-Br) did exhibit significant antibacterial activity against both bacterial strains with *S. aureus* (103.95 ppm) and *E. coli* (112.40 ppm), which is comparable to ampicillin for *E. coli*. The promising antibacterial activity of bromine substituted compound could be due to its molecular size and polarization ability leading to the formation of *van der Waals* interactions with the DNA of microbes [99].

Molecular docking

The compounds with minimum inhibitory concentration (MIC) below 200 ppm were further subjected to molecular docking analysis in order to identify the interactions attributed to the activities [100]. By using Schrodinger Maestro software (version 13.7.125), UDP-N-acetylmuramyl-tripeptide synthetase (MurE) (PDB ID: 7B6M) and Exogenous Dihydrofolate Reductase (DHFR) (PDB ID: 2W9S) enzymes were chosen to represent *E. coli* and *S.aureus* respectively whereby the binding affinity obtained were compared to standard ampicillin and cocrystal ligands. The relevance of choosing the MurE enzyme was due to its substantial function in the synthesis of cell walls [101] while DHFR plays a role as NADPH-dependent catalyzed which is significant in the biosynthesis of various key metabolites [102]. The binding sites were then identified by selecting SZN and TOP co-crystals in MurE and DHFR proteins, respectively, based on the Schrodinger Receptor Grid Generation module. This parameter validation is important to set the docking [103] occurring in the stipulated binding pockets as in **Figure 1**. The binding scores obtained are tabulated in **Table 5**.

Based on the *in vitro* MIC data, compounds **2** (*o*-F), **3** (*m*-F), **4** (*p*-F), **6** (*m*-Cl) and **9** (*m*-Br) were docked to the MurE enzyme and gave a binding affinity in the range of –7.24 to –8.32 kcal/mol that is higher than ampicillin (–6.92 kcal/mol). The presence of hydrogen bonding, *van der Waals*, π–π stacked, π–π T-shaped and π–alkyl interactions are the key contributions to the binding scores [104]. The slightly higher binding energies of the compounds than ampicillin was attributed to the more amino acid residues such as GLY246, ILE239 and VAL94, which are similar to those interacting with the SZN cocrystal. Apart, compound **4** (*p*-F) with the highest binding affinity (–8.32 kcal/mol) portrayed a similar water hydrogen bonding interaction with HOH779 residue as in the SZN cocrystal. While the 2D interactions diagram can be retrieved from the **S78** (Supplementary file), **Figure 2** depicted the 2D interactions of compound **4** (*p*-F) as a representative, SZN cocrystal and ampicillin.

Towards DHFR protein, all compounds except compounds **4** (*p*-F), **10** (*p*-Br), **11** (*o*-OCH_3) and **13** (*p*-OCH_3) were docked whereby binding scores of –6.75 to –8.01 kcal/mol were obtained. Contrary to the previous, ampicillin possessed a commendable binding affinity of –7.48 kcal/mol which is slightly higher than compounds **1** (H) and **9** (*m*-Br) scoring –6.75 kcal/mol and–7.44 kcal/mol respectively (**Figure 3**). This result is potentially due to the multiple hydrogen bonding shown by ampicillin with GLY93 and TYR98, whereas the compounds only showed one hydrogen bonding from the OH of phenol with ASN18 residue. An increases in the hydrogen bonding interaction significantly improves the binding affinity by increasing the solvation capacity of the compound in the biological system [105,106]. In addition, all docked compounds also displayed *van der Waals* and various hydrophobic interactions including alkyl, π–alkyl and others (see Supplementary File **S79**) with amino acid residues in the vicinity.

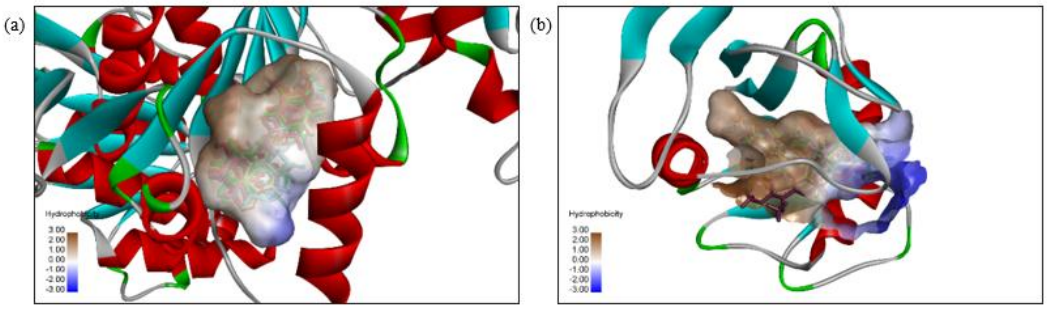

Figure 1. (a) Docked ligand in the binding pocket of MurE and **(b)** Docked ligand in the binding pocket of DHFR

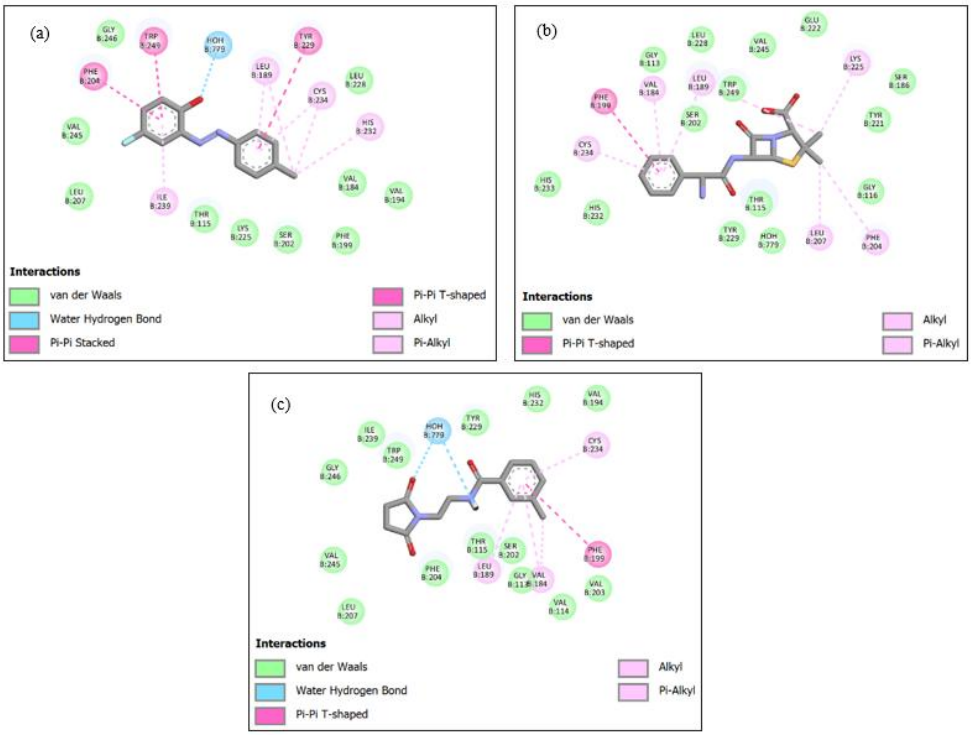

Figure 2. 2D diagram of **(a)** Compounds **4** (*p*-F) **(b)** ampicillin and **(f)** Cocrystal SZN docked to MurE protein visualized by Discovery Studio 2024

Table 5. Binding affinity for compounds with MIC <200 ppm

Compound	Binding affinity (Kcal/mol)	
	***E. coli* (MurE)**	***S. aureus* (DPHR)**
1 (H)	/	-6.75
2 (*o*-F)	-7.62	-8.01
3 (*m*-F)	-7.68	-7.80
4 (*p*-F)	-8.32	/
5 (*o*-Cl)	/	-7.93
6 (*m*-Cl)	-7.24	-7.55
7 (*p*-Cl)	/	-7.77
8 (*o*-Br)	/	-7.98
9 (*m*-Br)	-7.35	-7.44
10 (*p*-Br)	/	/
11 (*o*-OCH_3)	/	/
12 (*m*-OCH_3)	/	-7.89
13 (*p*-OCH_3)	/	/
Ampicillin	-6.92	-7.48
Cocrystal	-8.00	-8.78

Note: (/) - not applicable

***In silico* ADMET pharmacokinetic prediction**

ADMET prediction was utilized as screening projection for the absorption (A), distribution (D), metabolism (M), excretion (E) and toxicity (T) properties by using *in silico* pkCSM [107]. The result obtained is tabulated in **S80** (Supplementary file). In absorption analysis, all compounds have shown moderate water solubility ranging from –3.974 log mol/L to –5.034 log mol/L and excellent Caco2 permeability with values higher than 0.9 log Papp in 10^{-6} cm/s except for compound **8** (*o*-Br) 0.544 log Papp in 10^{-6} cm/s [108]. Most compounds have shown more than 90% intestinal absorption and excellent skin permeability of a Log Kp more than –2.5 [109]. In relation to the distribution aspect, the compounds have shown moderate blood-brain barrier permeability and moderate volume distribution [44] while high central nervous system permeability of more than –2.0 log PS [108]. In terms of the metabolism screening, the compounds were able to inhibit three cytochromes of CYP1A2, CYP2C19 and CYP2C9 [110–112] that obstruct the elimination of drugs from the body [113] while CYP2D6 and CYP3A4 were not inhibited. Pertaining to the excretion, the compounds were not able to be excreted by the renal organic cation transporter 2 (OCT2) [114] and were observed to have slow total clearance of compounds from the body. Lastly, most of the compounds found to be positive for AMES toxicity which can be potentially mutagenic except for compound **8** (*o*-Br) [115]. However, the compounds were expected to have a maximum tolerated dose amount of 0.422 to 1.046 log mg/kg/day in humans. In conjunction with that, the compounds are expected to be safe for humans as they were not active as hERG I inhibitors, hERG II inhibitors, hepatotoxicity and skin sensitization [116] with a Minnow toxicity score of lower than log 05 mM which is considered as non-toxic [117] except for compound **1** (H) is expected to have skin sensitization.

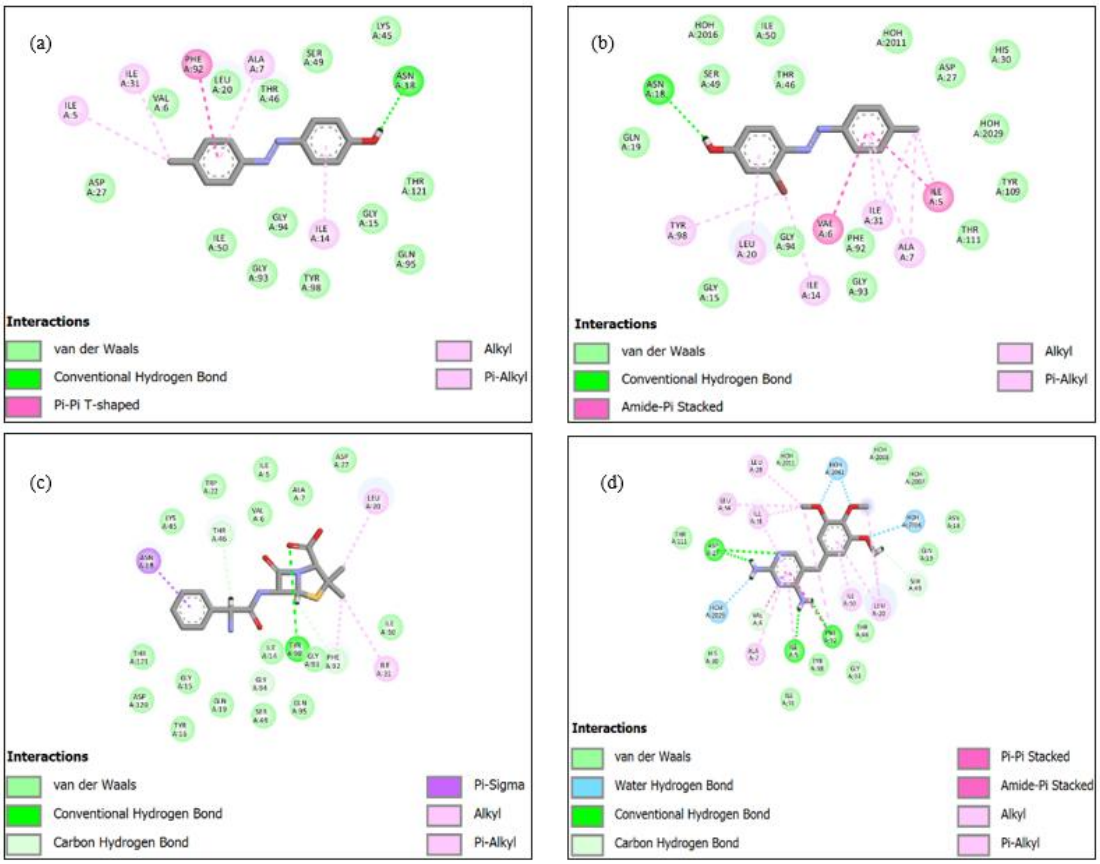

Figure 3. 2D diagram of **(a)** Compounds **1** (H) **(b) 9** (*m*-Br) **(c)** ampicillin and **(f)** Cocrystal TOP docked to DPHR protein visualized by Discovery Studio 2024

Conclusion

A series of *p*-toluidine azo derivatives bearing halogen and methoxy substituent **1-13** were successfully synthesized and evaluated with their biological potential. Compound **11** (*o*-OCH_3) has shown the most promising antioxidant activity

when tested against DPPH assay with an IC_{50} value of 25.5 ppm while compound **13** has shown the highest activity when tested against FRAP assay with 182.73 mg/ml Trolox equivalent. Whereas, in the antibacterial study, the compounds have shown better inhibition activity against gram-positive bacteria (*S. aureus*) than gram-negative bacteria (*E. coli*) potentially due to the difference in the bacterial cell wall composition. A significant inhibitory action was shown by compound **3** (*m*-F), which possessed the lowest MIC value probably due to the small fluoro atom providing a larger inductive effect that led to the enhancement of activity. Notably, the other *meta*-substituted compounds have also shown promising inhibitory activities specifically toward *S. aureus*. Structural activity relationship through molecular docking of compounds with activities indicated that hydrogen bonding and various hydrophobic interactions contribute to increasing the binding affinity led to activities enhancement. Last but not least, the pharmacokinetics analysis on compounds **1-13** portrayed acceptable results with some dosage control needed for certain compounds.

Acknowledgement
The authors would like to thank and appreciate the Faculty of Resource Science and Technology (FRST), Universiti Malaysia Sarawak (UNIMAS) and Dr Ngieng Ngui Sing for providing the research facilities, assistance and expertise.

Conflict of interest
The authors declare that we do have a conflict of interest with respect to this manuscript.

Funding
The authors would like to acknowledge the Ministry of Higher Education Malaysia for providing the Fundamental Research Grant Scheme (FRGS) fund FRGS/1/2021/ STG01/UNIMAS/03/2 to complete this study.

Authors Contribution
The research design, funding acquisition and project conception were carried out by ANAH, ZN and SP. Experimental work was conducted by YKW, SP and DND while the *in silico* molecular docking analysis was carried out by NHZ, AHS and BRPK. YKW, ANAH, NHZ and AHS wrote, reviewed, edited and finalized the manuscript. The published version of the paper has been read and approved by all the authors.

References

1. Salam, M. A., Al-Amin, M. Y., Salam, M. T., Pawar, J. S., Akhter, N., Rabaan, A. A., and Alqumber, M. A. A. (2023). Antimicrobial resistance: A growing serious threat for global public health. *Healthcare*, 11(13): 1946.
2. Vidovic, N., and Vidovic, S. (2020). Antimicrobial resistance and food animals: Influence of livestock environment on the emergence and dissemination of antimicrobial resistance. *Antibiotics*, 9(2): 52.
3. Samreen, Ahmad, I., Malak, H. A., and Abulreesh, H. H. (2021). Environmental antimicrobial resistance and its drivers: A potential threat to public health. *Journal of Global Antimicrobial Resistance*, 27: 101-111.
4. Wilson, D. N., Hauryliuk, V., Atkinson, G. C., and O'Neill, A. J. (2020). Target protection as a key antibiotic resistance mechanism. *Nature Reviews Microbiology*, 18(11): 637-648.
5. Hasan, T. H., and Al-Harmoosh, R. A. (2020). Mechanisms of antibiotics resistance in bacteria. *Systematic Reviews in Pharmacy*, 11(6): 817-823.
6. Chen, H., Yang, J., Huang, C., Chen, C., and Chen, Y. (2024). Antibacterial activities of functional groups on the benzene rings in nucleic acid nanocarriers. *Materials Today Chemistry*, 2024: 4692043.
7. Kobisy, A. S., Nassar, H. N., Tawfik, S. M., Elshatoury, E. H., and Aiad, I. (2021). Mitigation of eco-unfriendly and costly microbial induced corrosion using novel synthesized Schiff base cationic surfactants. *Journal of Chemical Technology and Biotechnology*, *96*(4): 941-952.
8. Joydeep, G., and Lavanya, L. M. (2023). Inhibition of microbial corrosion by green inhibitors: An overview. *Iranian Journal of Chemistry and Chemical Engineering*, *42*(2): 684-703.
9. Rao, P., and Mulky, L. (2023). Microbially influenced corrosion and its control measures: A critical review. *Journal of Bio- and Tribo-Corrosion*, 9(3): 57.
10. Mezgebe, K., and Mulugeta, E. (2022). Synthesis and pharmacological activities of azo dye derivatives incorporating heterocyclic scaffolds: A review. *RSC Advances*, 12(40): 25932-25946.
11. Dong, L., Chen, Y., Zhai, F., Tang, L., Gao, W., Tang, J., Feng, Y., and Feng, W. (2020). Azobenzene-based solar thermal energy storage enhanced by gold nanoparticles for rapid, optically-triggered heat release at room temperature. *Journal of Materials Chemistry A*, *8*(36): 18668-18676.
12. Bukia, T., Utiashvili, M., Tsiskarishvili, M., Jalalishvili, S., Gogolashvili, A., Tatrishvili,

T., and Petriashvili, G. (2023). Synthesis of some azo dyes based on 2,3,3-Trimethyl-3H-Indolenine. *Chemistry and Chemical Technology*, 17(3): 549-556.

13. Tahir, T., Shahzad, M. I., Tabassum, R., Rafiq, M., Ashfaq, M., Hassan, M., Kotwica-Mojzych, K., and Mojzych, M. (2021). Diaryl azo derivatives as anti-diabetic and antimicrobial agents: Synthesis, *in vitro*, kinetic and docking studies. *Journal of Enzyme Inhibition and Medicinal Chemistry*, 36(1): 1508-1519.
14. Gičević, A., Hindija, L., & Karačić, A. (2020). Toxicity of azo dyes in pharmaceutical industry. *IFMBE Proceedings*, *73*: 581-587.
15. Mughal, E. U., Raja, Q. A., Alzahrani, A. Y. A., Naeem, N., Sadiq, A., and Bozkurt, E. (2023). Pyrimidine-based azo dyes: Synthesis, photophysical investigations, solvatochromism explorations and anti-bacterial activity. *Dyes and Pigments*, 220(8): 111762.
16. Wencewicz, T. A. (2019). Crossroads of antibiotic resistance and biosynthesis. *Journal of Molecular Biology*, 431(18): 3370-3399.
17. Biswal, D., Jha, A., & Sen, A. (2021). Screening donor and acceptor groups for organic azo-based dyes for dye sensitized solar cells. *Journal of Molecular Structure*, 1228: 129776.
18. Oyetade, J. A., Machunda, R. L., and Hilonga, A. (2022). Photocatalytic degradation of azo dyes in textile wastewater by Polyaniline composite catalyst-a review. *Scientific African*, 17: e01305.
19. Rodriguez, F., Jelken, J., Delpouve, N., Laurent, A., Garnier, B., Duvail, J. L., Lagugné-Labarthet, F., and Ishow, E. (2021). Exploiting light interferences to generate micrometer-high superstructures from monomeric azo materials with extensive orientational mobility. *Advanced Optical Materials*, *9*(19): 2100525.
20. Yu, Q., Li, F., Yin, P., Pang, S., Staples, R. J., and Shreeve, J. M. (2021). Bridged and fused triazolic energetic frameworks with an azo building block towards thermally stable and applicable propellant ingredients. *Journal of Materials Chemistry A*, *9*(44): 24903-24908.
21. Saxena, A., and Gupta, S. (2020). Bioefficacies of microbes for mitigation of azo dyes in textile industry effluent: A review. *BioResources*, 15(4): 9858-9881.
22. Kamoon, R. A., Jawad Al-Mudhafar, M. M., and Omar, T. N. A. (2020). Synthesis, characterization and antimicrobial evaluation of new azo compounds derived from sulfonamides and isatin Schiff base. *International Journal of Drug Delivery Technology*, 10(1): 150-155.
23. Park, J., and Cheon, J. H. (2022). Updates on conventional therapies for inflammatory bowel diseases: 5-aminosalicylates, corticosteroids, immunomodulators, and anti-TNF-α. *Korean Journal of Internal Medicine*, 37(5): 895-905.
24. Crouwel, F., Buiter, H. J. C., and De Boer, N. K. (2021). Gut microbiota-driven drug metabolism in inflammatory bowel disease. *Journal of Crohn's and Colitis*, 15(2): 307-315.
25. Otkur, W., Wang, J., Hou, T., Liu, F., Yang, R., Li, Y., Xiang, K., Pei, S., Qi, H., Lin, H., Zhou, H., Zhang, X., Piao, H. long, and Liang, X. (2023). Aminosalicylates target GPR35, partly contributing to the prevention of DSS-induced colitis. *European Journal of Pharmacology*, 949: 175719.
26. Cerón-Carrasco, J. P., and Jacquemin, D. (2021). Using theory to extend the scope of azobenzene drugs in chemotherapy: Novel combinations for a specific delivery. *ChemMedChem*, 16(11): 1765-1775.
27. O'Reilly, C., Mills, S., Rea, M. C., Lavelle, A., Ghosh, S., Hill, C., and Ross, R. P. (2023). Interplay between inflammatory bowel disease therapeutics and the gut microbiome reveals opportunities for novel treatment approaches. *Microbiome Research Reports*, 2(4): 35.
28. Cheng, H. B., Zhang, S., Qi, J., Liang, X. J., and Yoon, J. (2021). Advances in application of azobenzene as a trigger in biomedicine: Molecular design and spontaneous assembly. *Advanced Materials*, 33(26): 2007290.
29. Kumar Trivedi, M., Branton, A., Trivedi, D., Nayak, G., and Singh, R. (2015). Characterization of physical, thermal and spectroscopic properties of biofield energy treated *p*-phenylenediamine and *p*-toluidine. *Journal of Environmental & Analytical Toxicology*, *5*(6): 1-10.
30. Obasuyi, E., and Iyekowa, O. (2019). Synthesis, characterization and antimicrobial of Schfiff Base from 5-Bromo – Salicylaldehyde and *p*-toluidine. *Journal of Applied Sciences and Environmental Management*, *22*(11): 1733.
31. Ngaini, Z., and Ho, B. K. (2017). Synthesis and antibacterial activity of azo and aspirin-azo derivatives. *Malaysian Journal of Analytical Sciences*, 21(5): 1183-1194.
32. Ge, W., Cao, S., Shen, F., Wang, Y., Ren, J., and Wang, X. (2019). Rapid self-healing,

stretchable, moldable, antioxidant and antibacterial tannic acid-cellulose nanofibril composite hydrogels. *Carbohydrate Polymers*, 224(7): 115147.

33. Olszowy, M. (2019). What is responsible for antioxidant properties of polyphenolic compounds from plants? *Plant Physiology and Biochemistry*, 144: 135-143.
34. Marinescu, M., Popa, C. V., Tănase, M. A., Soare, A. C., Tablet, C., Bala, D., Cinteza, L. O., Diţu, L. M., Gifu, I. C., and Petcu, C. (2022). Synthesis, characterization, DFT study and antifungal activities of some novel 2-(Phenyldiazenyl)phenol based azo dyes. *Materials*, 15(22): 8162.
35. Ribeiro, A. I., Dias, A. M., and Zille, A. (2022). Synergistic effects between metal nanoparticles and commercial antimicrobial agents: A review. *ACS Applied Nano Materials*, *5*(3): 3030-3064.
36. Abd Halim, A. N., Mohammad Hussin, A. S., Ngaini, Z., Zamakshshari, N. H., and Haron, I. Z. (2023). Synthesis, antibacterial potential and in silico molecular docking analysis of triazene compounds via diazo coupling reactions of an amine. *Tetrahedron Letters*, 132: 154803.
37. Frías-Moreno, M. N., Parra-Quezada, R. A., González-Aguilar, G., Ruíz-Canizales, J., Molina-Corral, F. J., Sepulveda, D. R., Salas-Salazar, N., and Olivas, G. I. (2021). Quality, bioactive compounds, antioxidant capacity, and enzymes of raspberries at different maturity stages, effects of organic vs. conventional fertilization. *Foods*, 10(5): 953.
38. Abd Halim, A. N., and Ngaini, Z. (2017). Synthesis and characterization of halogenated bis(acylthiourea) derivatives and their antibacterial activities. *Phosphorus, Sulfur and Silicon and the Related Elements*, 192(9): 1012-1017.
39. Muddassir, M., Raza, A., Munir, S., Basirat, A., Ahmed, M., Butt, M. S., Dar, O. A., Ahmed, S. S., Shamim, S., and Naqvi, S. Z. H. (2022). Antibacterial efficacy of silver nanoparticles (AgNPs) against metallo-β-lactamase and extended spectrum β-lactamase producing clinically procured isolates of Pseudomonas aeruginosa. *Scientific Reports*, 12(1): 1-16.
40. Muddagoni, N., Bathula, R., Dasari, M., and Potlapally, S. R. (2021). Homology modeling, virtual screening, prime-mmgbsa, autodock-identification of inhibitors of fgr protein. *Biointerface Research in Applied Chemistry*, 11(4): 11088-11103.
41. Kumar, Ashutosh, and Zhang, K. Y. J. (2013). Investigation on the effect of key water molecules on docking performance in CSARdock exercise. *Journal of Chemical Information and Modeling*, 53(8): 1880-1892.
42. Owoloye, A. J., Ligali, F. C., Enejoh, O. A., Musa, A. Z., Aina, O., Idowu, E. T., and Oyebola, K. M. (2022). Molecular docking, simulation and binding free energy analysis of small molecules as Pf HT1 inhibitors. *PLoS ONE*, 17(7): 1-18.
43. Alogheli, H., Olanders, G., Schaal, W., Brandt, P., and Karlén, A. (2017). Docking of macrocycles: comparing rigid and flexible docking in glide. *Journal of Chemical Information and Modeling*, *57*(2): 190-202.
44. Islam, A. U., Hadni, H., Ali, F., Abuzreda, A., and Kawsar, S. M. A. (2024). Synthesis, antimicrobial activity, molecular docking, molecular dynamics simulation, and ADMET properties of the mannopyranoside derivatives as antimicrobial agents. *Journal of Taibah University for Science*, 18(1): 2327101.
45. Smołka, S., and Krukiewicz, K. (2023). Catalyst design through grafting of diazonium salts—A critical review on catalyst stability. *International Journal of Molecular Sciences*, 24(16): 12575.
46. Firth, J. D., and Fairlamb, I. J. S. (2020). A need for caution in the preparation and application of synthetically versatile aryl diazonium tetrafluoroborate salts. *Organic Letters*, *22*(18): 7057-7059.
47. Mitrović, A., Wild, S., Lloret, V., Fickert, M., Assebban, M., Márkus, B. G., Simon, F., Hauke, F., Abellán, G., and Hirsch, A. (2021). Interface amorphization of two-dimensional black phosphorus upon treatment with diazonium salts. *Chemistry - A European Journal*, *27*(10): 3361-3366.
48. Schotten, C., Leprevost, S. K., Yong, L. M., Hughes, C. E., Harris, K. D. M., and Browne, D. L. (2020). Comparison of the thermal stabilities of diazonium salts and their corresponding triazenes. *Organic Process Research and Development*, *24*(10): 2336-2341.
49. Malík, I., Bukovský, M., Andriamainty, F., and Gališinová, J. (2013). Antimicrobial effect of para-alkoxyphenylcarbamic acid esters containing substituted N-phenylpiperazine moiety. *Brazilian Journal of Microbiology*, 44: 457-463.
50. Ngaini, Z., Rasin, F., Wan Zullkiplee, W. S. H., and Abd Halim, A. N. (2020). Synthesis and molecular design of mono aspirinate thiourea-azo hybrid molecules as potential antibacterial agents. *Phosphorus, Sulfur and Silicon and the Related Elements*, 196(3): 275-282.

51. Ravi, B. N., J, K., M, M. N., Kumar, V., & Kandgal, S. (2020). Synthesis, characterization and pharmacological evaluation of 2-aminothiazole incorporated azo dyes. *Journal of Molecular Structure*, 1204: 127493.
52. Bugakov, M., Boiko, N., Abramchuk, S., Zhu, X., and Shibaev, V. (2020). Azobenzene-containing liquid crystalline block copolymer supramolecular complexes as a platform for photopatternable colorless materials. *Journal of Materials Chemistry C*, *8*(4): 1225-1230.
53. He, S., Tang, M., Zhang, Z., Liu, H., Luo, M., and Sun, H. (2020). Hypoglycemic effects of phenolic compound-rich aqueous extract from water dropwort (Oenanthe javanica DC.) on streptozotocin-induced diabetic mice. *New Journal of Chemistry*, 44(14): 5190-5200.
54. Liu, Y., Long, S., Zhang, S., Tan, Y., Wang, T., Wu, Y., Jiang, T., Liu, X., Peng, D., and Liu, Z. (2021). Synthesis and antioxidant activities of berberine 9-O-benzoic acid derivatives. *RSC Advances*, 11(29):17611-17621.
55. Dey, K. K., and Ghosh, M. (2020). Determination of chemical shift anisotropy tensor and molecular correlation time of proton pump inhibitor omeprazole by solid state NMR measurements. *New Journal of Chemistry*, 44(44): 19393-19403.
56. Novakovic, M., Battistel, M. D., Azurmendi, H. F., Concilio, M. G., Freedberg, D. I., and Frydman, L. (2021). The incorporation of labile protons into multidimensional NMR analyses: Glycan structures revisited. *Journal of the American Chemical Society*, 143(23): 8935-8948.
57. Cihang Yu. (2022). *Exploring the Properties of Selectively Fluorinated Janus Cyclohexane Rings*. University of St Andrews.
58. Nizar, S. N. A. M., Ab Rahman, S. N. F., Zaini, M. F., Anizaim, A. H., Abdul Razak, I., and Arshad, S. (2020). The photovoltaic performance of sensitizers for organic solar cells containing fluorinated chalcones with different halogen substituents. *Crystals*, 11(11): 1357.
59. Al-Salami, B. K., Hameed, A. J., and Al-Rubaie, A. Z. (2021). Synthesis, antimicrobial, antioxidant and structural studies of some new sulfa drug containing an azo-azomethine group. *Egyptian Journal of Chemistry*, 64(2): 751-759.
60. El-Lateef, H. M. A., El-Dabea, T., Khalaf, M. M., and Abu-Dief, A. M. (2023). Recent overview of potent antioxidant activity of coordination compounds. *Antioxidants*, 12(2): 213.
61. Al Zahrani, N. A., El-Shishtawy, R. M., Elaasser, M. M., and Asiri, A. M. (2020). Synthesis of novel chalcone-based phenothiazine derivatives as antioxidant and anticancer agents. *Molecules*, *25*(19): 1-15.
62. Muğlu, H., Çavuş, M. S., Bakır, T. K., and Yakan, H. (2022). Synthesis of new bis(thiosemicarbazone) derivatives and DFT analysis of antioxidant characteristics in relation to HAT and SET reactions. *Journal of the Indian Chemical Society*, *99*(12), 100789.
63. Setiawan, V., Phangestu, S., Grace Soetikno, A., Arianti, A., and Kohar, I. (2021). Rapid screening analysis of antioxidant activities in green tea products using DPPH and FRAP. *Pharmaceutical Journal of Indonesia*, *7*(1): 9-14.
64. Peng, Z., Wang, G., Zeng, Q. H., Li, Y., Wu, Y., Liu, H., Wang, J. J., and Zhao, Y. (2021). Synthesis, antioxidant and anti-tyrosinase activity of 1,2,4-triazole hydrazones as antibrowning agents. *Food Chemistry*, 341: 128265.
65. Alfieri, M. L., Moccia, F., D'errico, G., Panzella, L., D'ischia, M., and Napolitano, A. (2020). Acid treatment enhances the antioxidant activity of enzymatically synthesized phenolic polymers. *Polymers*, 12(11): 2544.
66. Parcheta, M., Świsłocka, R., Orzechowska, S., Akimowicz, M., Choińska, R., and Lewandowski, W. (2021). Recent developments in effective antioxidants: The structure and antioxidant properties. *Materials*, 14(8): 1984.
67. Ingole, V. V., Mhaske, P. C., and Katade, S. R. (2022). Phytochemistry and pharmacological aspects of Tridax procumbens (L.): A systematic and comprehensive review. *Phytomedicine Plus*, *2*(1): 100199.
68. Marchi, R. C., Campos, I. A. S., Santana, V. T., and Carlos, R. M. (2022). Chemical implications and considerations on techniques used to assess the in vitro antioxidant activity of coordination compounds. *Coordination Chemistry Reviews*, 451: 214275.
69. Benzie, I. F. F., and Devaki, M. (2018). The ferric reducing/antioxidant power (FRAP) assay for non-enzymatic antioxidant capacity: Concepts, procedures, limitations and applications. *Measurement of Antioxidant Activity and Capacity: Recent Trends and Applications*, 77-106.

70. Abdellatif, A. A. H., Alhathloul, S. S., Aljohani, A. S. M., Maswadeh, H., Abdallah, E. M., Hamid Musa, K., & El Hamd, M. A. (2022). Green synthesis of silver nanoparticles incorporated aromatherapies utilized for their antioxidant and antimicrobial activities against some clinical bacterial isolates. *Bioinorganic Chemistry and Applications*, *2022*(1): 2432758.
71. Gulcin, İ. (2020). Antioxidants and antioxidant methods: An updated overview. *Archives of Toxicology*, 94(3): 651-715.
72. Barcena, H. S., Chen, P., and Tuachi, A. (2015). Synthetic anthocyanidins and their antioxidant properties. *SpringerPlus*, 4(1): 4–8.
73. Shakir, R. M., Jasim, H. S., Saoud, S. A., Hussain, D. F., and Ali, K. F. (2022). Synthesis, antioxidant, antibacterial and docking structure of new dihydro-pyrimidine derivatives containing multi phenol. *Journal of Pharmaceutical Negative Results*, 13(2): 57-68.
74. Halim, A. N., Yeo, K. W., Zamakshshari, N. H., Phornvillay, S., Ngaini, Z., and Diosing, D. N. (2024). Preparation, *in vitro* and *in silico* antioxidant and antibacterial studies of 4-aminoacetanilide azo derivatives. *Journal of the Indian Chemical Society*, 101(11): 101341.
75. Farmanzadeh, D., and Najafi, M. (2016). Novel trolox derivatives as antioxidants: A DFT investigation. *Journal of the Serbian Chemical Society*, 81(3): 277-290.
76. Yang, J., Chen, J., Hao, Y., and Liu, Y. (2021). Identification of the DPPH radical scavenging reaction adducts of ferulic acid and sinapic acid and their structure-antioxidant activity relationship. LWT, 146: 111411.
77. Chen, J., Yang, J., Ma, L., Li, J., Shahzad, N., & Kim, C. K. (2020). Structure-antioxidant activity relationship of methoxy, phenolic hydroxyl, and carboxylic acid groups of phenolic acids. *Scientific Reports*, 10(1): 2611.
78. Witwit, I. N., and Al-Waili, M. K. (2021). New azo ligand synthesis, characterization, and bacterial inhibition investigation as a derivative of 4,5-diphenylimidazole with some transition metal ions. *International Journal of Drug Delivery Technology*, 11(4): 1251-1257.
79. Ahghari, M. R., Soltaninejad, V., and Maleki, A. (2020). Synthesis of nickel nanoparticles by a green and convenient method as a magnetic mirror with antibacterial activities. *Scientific Reports*, 10(1): 1-10.
80. Liew, S. K., Malagobadan, S., Arshad, N. M., and Nagoor, N. H. (2020). A review of the structure—activity relationship of natural and synthetic antimetastatic compounds. *Biomolecules*, 10(1): 138.
81. Batovska, D., Parushev, S., Stamboliyska, B., Tsvetkova, I., Ninova, M., and Najdenski, H. (2009). Examination of growth inhibitory properties of synthetic chalcones for which antibacterial activity was predicted. *European Journal of Medicinal Chemistry*, 44(5): 2211-2218.
82. Moreno, L., Párraga, J., Galán, A., Cabedo, N., Primo, J., and Cortes, D. (2012). Synthesis of new antimicrobial pyrrolo[2,1-a]isoquinolin-3-ones. *Bioorganic and Medicinal Chemistry*, *20*(22): 6589-6597.
83. Kosikowska, U., Wujec, M., Trotsko, N., Płonka, W., Paneth, P., & Paneth, A. (2021). Antibacterial activity of fluorobenzoylthiosemicarbazides and their cyclic analogues with 1,2,4-triazole scaffold. *Molecules*, 26(1): 170.
84. Domínguez, A. V., Algaba, R. A., Canturri, A. M., Villodres, Á. R., and Smani, Y. (2020). Antibacterial activity of colloidal silver against gram-negative and gram-positive bacteria. *Antibiotics*, 9(1): 36.
85. Pohan, J., and Rahmawati, F. (2022). The effect of mangosteen pericarp (*Garcinia mangostana* Linn) extract on inhibits the growth of bacteria *Escherichia coli* ATCC 25922 and bacteria *Staphylococcus aureus* ATCC 25923. *International Journal of Research in Pharmacy and Pharmaceutical Sciences*, *7*(2): 29-38.
86. Luo, Z., Yue, S., Chen, T., She, P., Wu, Y., and Wu, Y. (2020). Reduced growth of *Staphylococcus aureus* under high glucose conditions is associated with decreased pentaglycine expression. *Frontiers in Microbiology*, 11: 537290.
87. Ortega-Buitrago, O., Chaves-Bedoya, G., and Ortiz-Rojas, L. Y. (2021). Chemical composition and antimicrobial activity of ethanolic bark and leave extract of Zanthoxylum Caribaeum Lam. from Norte de Santander, Colombia. *Revista de Chimie*, *72*(4): 152-161.
88. Sinsinwar, S., and Vadivel, V. (2020). Catechin isolated from cashew nut shell exhibits antibacterial activity against clinical isolates of MRSA through ROS-mediated oxidative stress. *Applied Microbiology and Biotechnology*, 104: 8279-8297.
89. Juariah, S., Bakar, F. I. A., Bakar, M. F. A., and Endrini, S. (2023). Antibacterial potential of *Curcuma caesia* Roxb ethanol extract against nosocomial infections. *Bali*

Medical Journal, 12(2): 1959-1963.

90. Kowalska-Krochmal, B., and Dudek-Wicher, R. (2021). The minimum inhibitory concentration of antibiotics: Methods, interpretation, clinical relevance. *Pathogens*, 10(2): 165.
91. Li, J., Rao, X., Shang, S., Gao, Y., & Song, J. (2012). Synthesis and antibacterial activity of amide derivatives from acrylopimaric acid. *BioResources*, *7*(2): 1961-1971.
92. Malladi, S., Nadh, R. V., Babu, K. S., and Babu, P. S. (2017). Synthesis and antibacterial activity studies of 2,4-di substituted furan derivatives. *Beni-Suef University Journal of Basic and Applied Sciences*, *6*(4): 345-353.
93. Mardirossian, M., Rubini, M., Adamo, M. F. A., Scocchi, M., Saviano, M., Tossi, A., Gennaro, R., and Caporale, A. (2021). Natural and synthetic halogenated amino acids—structural and bioactive features in antimicrobial peptides and peptidomimetics. *Molecules*, 26(23): 7401.
94. Al-Wahaibi, L. H., Alagappan, K., Gomila, R. M., Blacque, O., Frontera, A., Percino, M. J., El-Emam, A. A., and Thamotharan, S. (2023). A combined crystallographic and theoretical investigation of noncovalent interactions in 1,3,4-oxadiazole-2-thione-N-Mannich derivatives: In vitro bioactivity and molecular docking. *RSC Advances*, 13(48): 34064-34077.
95. Cañete-Molina, Á., Espinosa-Bustos, C., González-Castro, M., Faúndez, M., Mella, J., Tapia, R. A., Cabrera, A. R., Brito, I., Aguirre, A., and Salas, C. O. (2018). Bromination-a versatile tool for drugs optimization. *The Medical-Surgical Journal*, 122(3): 614-626.
96. Kanwal, Khan, K. M., Chigurupati, S., Ali, F., Younus, M., Aldubayan, M., Wadood, A., Khan, H., Taha, M., and Perveen, S. (2021). Indole-3-acetamides: As potential antihyperglycemic and antioxidant agents; synthesis, *in vitro* α-amylase inhibitory activity, structure-activity relationship, and *in silico* studies. *ACS Omega*, *6*(3): 2264-2275.
97. Olchowik-Grabarek, E., Sękowski, S., Kwiatek, A., Płaczkiewicz, J., Abdulladjanova, N., Shlyonsky, V., Swiecicka, I., and Zamaraeva, M. (2022). The structural changes in the membranes of *Staphylococcus aureus* caused by hydrolysable tannins witness their antibacterial activity. *Membranes*, 12: 1124.
98. Das, A., Das, A., and Banik, B. K. (2021). Influence of dipole moments on the medicinal activities of diverse organic compounds. *Journal of the Indian Chemical Society*, *98*(2): 100005.
99. Kuzey, N. G., Özgür, M., Cemaloğlu, R., Asmafiliz, N., Kılıç, Z., Açık, L., Aydın, B., and Hökelek, T. (2020). Mono- and dispirocyclotriphosphazenes containing 4-bromobenzyl pendant arm(s): Synthesis, spectroscopy, crystallography and biological activity studies. *Journal of Molecular Structure*, 1220: 128658.
100. Rashdan, H. R. M., Shehadi, I. A., and Abdelrahman, M. T. (2021). Antibacterial activities and molecular docking of novel sulfone biscompound containing bioactive 1,2,3-triazole moiety. *Molecules*, 26(16): 4817.
101. Kumar, Ankit, Singh, P., Singh, E., Jain, M., Muthukumaran, J., and Singh, A. K. (2024). *In silico* strategies for identifying therapeutic candidates against *Acinetobacter baumannii*: Spotlight on the UDP-N-acetylmuramoyl-L-alanine-D-gluta mate:meso-diaminopimelate ligase (MurE). *Journal of Biomolecular Structure and Dynamics*, 1-15.
102. Aragaw, W. W., Negatu, D. A., Bungard, C. J., Dartois, V. A., Marrouni, A. El, Elliott, B., Olsen, D. B., Warrass, R., and Dick, T. (2024). *Pharmacological validation of dihydrofolate reductase as a drugtarget in Mycobacterium abscessus*. 68(1): e00717-23.
103. Muzaffar-Ur-Rehman, M., Suryakant, C. K., Chandu, A., Kumar, B. K., Joshi, R. P., Jadav, S. R., Sankaranarayanan, M., and Vasan, S. S. (2024). Molecular docking and dynamics identify potential drugs to be repurposed as SARS-CoV-2 inhibitors. *Journal of Computational Biophysics and Chemistry*, 1-23.
104. Shawon, J., Khan, A. M., Shahriar, I., & Halim, M. A. (2021). Improving the binding affinity and interaction of 5-Pentyl-2-Phenoxyphenol against Mycobacterium Enoyl ACP reductase by computational approach. *Informatics in Medicine Unlocked*, 23: 100528.
105. Kortemme, T., Morozov, A. V., and Baker, D. (2003). An orientation-dependent hydrogen bonding potential improves prediction of specificity and structure for proteins and protein-protein complexes. *Journal of Molecular Biology*, 326(4): 1239-1259.
106. Chen, D., Oezguen, N., Urvil, P., Ferguson, C., Dann, S. M., and Savidge, T. C. (2016). Regulation of protein-ligand binding affinity by hydrogen bond pairing. *Science Advances*, *2*(3): e1501240.
107. Kamel, M. S., Belal, A., Aboelez, M. O.,

Shokr, E. K., Abdel-Ghany, H., Mansour, H. S., Shawky, A. M., and El-Remaily, M. A. E. A. A. A. (2022). Microwave-assisted synthesis, biological activity evaluation, molecular docking, and ADMET studies of some novel pyrrolo [2,3-b] pyrrole derivatives. *Molecules*, *27*(7): 2061.

108. Hanee, U., Rahman, M. R., and Matin, M. M. (2021). Synthesis, PASS, *in silico* ADMET and thermodynamic studies of some galactopyranoside esters. *Physical Chemistry Research*, 9(4): 591-603.
109. dos Santos, K. L., Marques, D. S. C., Jacob, I. T., da Silva, P. R., Machado, D. C., Souza, T. R. C. L., de Oliveira, J. F., Almeida, S. M. V., Filho, I. J. da C., and de Lima, M. do C. A. (2024). *In silico* prediction of ADMET parameters and *in vitro* evaluation of antioxidant and cytotoxic activities promoted by indole-thiosemicarbazone compounds. *Anais Da Academia Brasileira de Ciencias*, *96*(3): e20230811.
110. Ito, J., Lemus, H., & Wu, T. (2023). Serum phosphorus, serum bicarbonate, and renal function in relation to liver CYP1A2 activity. *Diagnostics*, 13(18): 2996.
111. de Jong, L. M., Boussallami, S., Sánchez-López, E., Giera, M., Tushuizen, M. E., Hoekstra, M., Hawinkels, L. J. A. C., Rissmann, R., Swen, J. J., and Manson, M. L. (2023). The impact of CYP2C19 genotype on phenoconversion by concomitant medication. *Frontiers in Pharmacology*, 14: 1201906.
112. Zhou, Y., Nevosadová, L., Eliasson, E., and Lauschke, V. M. (2023). Global distribution of functionally important CYP2C9 alleles and their inferred metabolic consequences. *Human Genomics*, 17(1): 15.
113. Daina, A., Michielin, O., and Zoete, V. (2017). SwissADME: A free web tool to evaluate pharmacokinetics, drug-likeness and medicinal chemistry friendliness of small molecules. *Scientific Reports*, *7*(1): 42717.
114. Chalkha, M., Nour, H., Chebbac, K., Nakkabi, A., Bahsis, L., Bakhouch, M., Akhazzane, M., Bourass, M., Chtita, S., Bin Jardan, Y. A., Augustyniak, M., Bourhia, M., Aboul-Soud, M. A. M., and El Yazidi, M. (2022). Synthesis, characterization, DFT mechanistic study, antimicrobial activity, molecular modeling, and ADMET properties of novel pyrazole-isoxazoline hybrids. *ACS Omega*, *7*(50): 46731-46744.
115. Çapan, İ., Hawash, M., Jaradat, N., Sert, Y., Servi, R., and Koca, İ. (2023). Design, synthesis, molecular docking and biological evaluation of new carbazole derivatives as anticancer, and antioxidant agents. *BMC Chemistry*, 17(1): 60.
116. Olaokun, O. O., and Zubair, M. S. (2023). Antidiabetic activity, molecular docking, and ADMET properties of compounds isolated from bioactive ethyl acetate fraction of ficus lutea leaf extract. *Molecules*, 28(23): 7717.
117. Klimoszek, D., Jeleń, M., Dołowy, M., & Morak-Młodawska, B. (2024). Study of the lipophilicity and ADMET parameters of new anticancer diquinothiazines with pharmacophore substituents. *Pharmaceutic als*, 17(6): 725.